Human Molecular Genetics, 2013, Vol. 22, No. 6 **1140–1156**
doi:10.1093/hmg/dds522
Advance Access published on December 13, 2012

GTPase activity regulates kinase activity and cellular phenotypes of Parkinson's disease-associated LRRK2

Alice Biosa[1,2], Alzbeta Trancikova[1,†], Laura Civiero[3], Liliane Glauser[1], Luigi Bubacco[3], Elisa Greggio[3] and Darren J. Moore[1,*]

[1]Brain Mind Institute, School of Life Sciences, Ecole Polytechnique Fédérale de Lausanne (EPFL), Lausanne 1015, Switzerland [2]Department of Clinical and Experimental Medicine, Medical School, University of Sassari, Sassari 07100, Italy and [3]Department of Biology, University of Padova, Padova 35121, Italy

Received October 3, 2012; Revised and Accepted December 9, 2012

Mutations in the *LRRK2* gene cause autosomal dominant Parkinson's disease. *LRRK2* encodes a multi-domain protein containing a Ras-of-complex (Roc) GTPase domain, a C-terminal of Roc domain and a protein kinase domain. LRRK2 can function as a GTPase and protein kinase, although the interplay between these two enzymatic domains is poorly understood. Although guanine nucleotide binding is critically required for the kinase activity of LRRK2, the contribution of GTP hydrolysis is not known. In general, the molecular determinants regulating GTPase activity and how the GTPase domain contributes to the properties of LRRK2 remain to be clarified. Here, we identify a number of synthetic missense mutations in the GTPase domain that functionally modulate GTP binding and GTP hydrolysis and we employ these mutants to comprehensively explore the contribution of GTPase activity to the kinase activity and cellular phenotypes of LRRK2. Our data demonstrate that guanine nucleotide binding and, to a lesser extent, GTP hydrolysis are required for maintaining normal kinase activity and both activities contribute to the GTP-dependent activation of LRRK2 kinase activity. Guanine nucleotide binding but not GTP hydrolysis regulates the dimerization, structure and stability of LRRK2. Furthermore, GTP hydrolysis regulates the LRRK2-dependent inhibition of neurite outgrowth in primary cortical neurons but is unable to robustly modulate the effects of the familial G2019S mutation. Our study elucidates the role of GTPase activity in regulating kinase activity and cellular phenotypes of LRRK2 and has important implications for the validation of the GTPase domain as a molecular target for attenuating LRRK2-mediated neurodegeneration.

INTRODUCTION

Mutations in the *leucine-rich repeat kinase 2* (*LRRK2*) gene are a common cause of late-onset, autosomal dominant familial Parkinson's disease (PD) (1–3). The *LRRK2* gene encodes a 2527 amino acid multi-domain protein containing a central catalytic region consisting of a Ras-of-complex (Roc) GTPase domain and a serine/threonine-directed protein kinase domain connected by a C-terminal of Roc (COR) domain (4). The Roc-COR tandem region of LRRK2 is characteristic of members of the ROCO protein family that in humans consists of four members, LRRK1, LRRK2, DAPK1 and MFHAS1 (5,6). LRRK2 also contains several regions implicated in protein–protein interactions including armadillo, ankyrin, leucine-rich and WD40 repeat domains. Similar to other small GTPases, the GTPase domain of LRRK2 binds guanine nucleotides via a phosphate-binding motif (P-loop) region (residues 1341–1348, GNTGSGKT) and can hydrolyze GTP, although at a slow rate, involving a catalytic Switch II motif (residues 1394–1398, DFAGR) (7–11). The Switch II motif of LRRK2 contains an Arg (R) residue at position 1398, whereas a similarly charged Gln

*To whom correspondence should be addressed at: Brain Mind Institute, Ecole Polytechnique Fédérale de Lausanne (EPFL), SV-BMI-LMNR, AI 2150, Station 19, 1015 Lausanne, Switzerland. Tel: +41 216930971; Email: darren.moore@epfl.ch
†Present address: UCB Pharma S.A., Chemin du Foriest, B–1420 Braine-l'Alleud, Belgium.

(Q) residue occupies the equivalent position in the majority of small GTPases and is critical for GTPase activity. In the related ROCO proteins LRRK1 and MFHAS1, the equivalent R1398 residue is substituted to Pro (DIGGP) or Asp (DLAGD), respectively (5,6), thereby suggesting a distinct mechanism of regulation of ROCO proteins compared with other small GTPase family members. Although a Q→L substitution in Ras GTPases results in a GTPase-inactive protein that is 'GTP-locked' and constitutively active, the equivalent R1398L substitution in LRRK2 oppositely enhances its GTPase activity (12,13). The identification of an equivalent 'GTP-locked' mutation in LRRK2 has so far proved elusive but will prove valuable for determining the structure and activity of LRRK2 in a presumably GTP-bound conformation. In general, the molecular determinants regulating the GTPase activity of LRRK2 remain poorly defined and how the GTPase domain functionally interacts with the kinase domain is incompletely understood. PD-related mutations in LRRK2 either lead to enhanced kinase activity (i.e. G2019S) or to reduced GTPase activity (i.e. R1441C, R1441G or Y1699C), suggesting that both kinase and GTPase activities are important for the development of PD due to *LRRK2* mutations (8,9,13–16). Furthermore, pathogenic mutations in LRRK2 promote neuronal toxicity through a guanine nucleotide-binding and kinase-dependent mechanism (10,11,16). Therefore, the GTPase domain represents a potentially promising molecular target for modulating LRRK2 activity and neuronal toxicity.

Small GTPases normally act as molecular switches that cycle between GTP-bound 'active' and GDP-bound 'inactive' states, with the GTP-bound state leading to the binding and activation of downstream effector proteins such as kinases, i.e. the activation of Raf kinase by Ras GTPase. For LRRK2, an intact GTPase domain is critically required for kinase activity since the disruption of guanine nucleotide binding by the introduction of P-loop null mutations (i.e. K1347A or T1348N) results in a kinase-inactive form of LRRK2 (10,11). Although guanine nucleotide binding appears to be critically required for the kinase activity of LRRK2, the relative contributions of GDP and GTP binding are unclear. The kinase activity of LRRK2 is enhanced by treatment of cell lysates with GTP or its analogs prior to LRRK2 purification, whereas the direct binding of GTP to purified LRRK2 *in vitro* fails to similarly enhance its kinase activity (11,17). These observations suggest that LRRK2 kinase activity can be influenced by the ability for GTP binding rather than by direct GTP binding and imply that an unidentified guanine nucleotide-binding protein could be required for the GTP-dependent kinase activation of LRRK2 that occurs in cells. Therefore, the relationship between the GTPase and kinase domains of LRRK2 does not initially appear to conform to a classical activation mechanism similar to the Ras-Raf pathway. At present, we understand little about the overall contribution of the GTPase domain to the enzymatic, biochemical and cellular properties of LRRK2. Accordingly, in the present study, we develop a collection of functional GTPase domain mutants that modulate GTP binding and hydrolysis to comprehensively explore the contribution of GTPase activity to the biochemical and cellular phenotypes of LRRK2.

RESULTS

Development of LRRK2 GTPase and kinase domain functional mutants

To begin to explore the contribution of the GTPase domain to the properties of LRRK2, we developed a panel of full-length FLAG-tagged human LRRK2 expression constructs containing a collection of synthetic mutations analogous to well-characterized functional residues in members of the Ras GTPase superfamily (Table 1). We introduced missense mutations in the P-loop motif that disrupt guanine nucleotide binding (K1347A, T1348N and G2019S/T1348N) (11), in the Switch II motif that are predicted to modulate GTP hydrolysis (R1398L, R1398L/T1343V and R1398Q/T1343G) (7,12,13), in the kinase domain that impair (K1906M, D1994A, D1994N, G2019S/K1906M, G2019S/D1994A and G2019S/D1994N) or enhance (G2019S) kinase activity (10,11,14,16), and various combinations of mutations of the GTPase domain together with kinase-inactive (D1994A/R1398L and D1994A/R1398L/T1343V) or kinase-enhanced (G2019S/R1398L and G2019S/R1398L/T1343V) variants (Fig. 1 and Table 1). We first analyzed the effects of each mutation on the steady-state levels of LRRK2 protein transiently expressed in HEK-293T cells. The majority of mutations produce similar steady-state levels of LRRK2 protein compared with wild-type (WT) LRRK2, although the P-loop mutations, K1347A and T1348N, cause a significant reduction of LRRK2 levels (Fig. 2A and B). Our data reveal that mutations in functional residues of the GTPase and kinase domains are generally well-tolerated and do not have major effects on the steady-state levels of LRRK2 protein, with the notable exception of P-loop mutations that are known to disrupt guanine nucleotide binding (11).

Identification of mutations that modulate LRRK2 GTP binding and GTP hydrolysis

We next sought to confirm the functional effects of these mutations on LRRK2 GTPase activity by conducting well-established assays to measure GTP binding and GTP hydrolysis (11–13). For assessments of GTP binding, pull-down assays were conducted with GTP-agarose on cell extracts expressing each LRRK2 variant to determine the relative level of GTP binding (Table 1). Compared with WT LRRK2, the K1347A, T1348N and G2019S/T1348N mutations which disrupt the guanine nucleotide-binding P-loop motif significantly impair the GTP binding of LRRK2 (Fig. 3A), as previously reported (11). Unexpectedly, the kinase-inactive forms of Switch II motif variants (D1994A/R1398L and D1994A/R1398L/T1343V) impair GTP binding to a degree similar to P-loop mutations (Fig. 3A). Kinase activity is not required for the normal GTP binding of LRRK2 as suggested by the normal GTP binding of kinase-inactive (i.e. K1906M, D1994A and D1994N) or kinase-enhanced (i.e. G2019S) mutants (Fig. 3A). These data demonstrate that an intact P-loop motif is critically required for normal GTP binding of LRRK2.

We next explored the effects of GTPase and kinase domain mutations on LRRK2-mediated GTP hydrolysis by measuring the release of free γ-phosphate from GTP (12,13). We first established time–response curves, using three known LRRK2 variants

Table 1. LRRK2 GTPase and kinase domain mutations and expected/observed functional effects

Mutation	Domain/motif	Expected effect (relative to WT LRRK2)	GTP binding (observed)	GTP hydrolysis (observed)	Kinase activity (observed)
T1343G	GTPase/P-loop	?	–	–	–
K1347A	GTPase/P-loop	Impaired guanine nucleotide binding	↓	↓	↓↓
T1348N	GTPase/P-loop	Impaired guanine nucleotide binding	↓↓	↓↓	↓↓
R1398L	GTPase/Switch II	Impaired GTP hydrolysis	–	↑↑	–/↓
R1398Q	GTPase/Switch II	Ras-like; enhanced GTP hydrolysis	–	–	–
K1906M	Kinase/ATP-binding site	Kinase-inactive	–	–	↓↓
D1994A	Kinase/proton-acceptor site	Kinase-inactive	–	–	↓↓
D1994N	Kinase/proton-acceptor site	Kinase-inactive	–	–	↓↓
G2019S	Kinase/activation loop	Enhanced kinase activity	–	–	↑↑
R1398L/T1343V	GTPase/P-loop and Switch II	Impaired GTP hydrolysis	–	↓↓	↓
R1398Q/T1343G	GTPase/P-loop and Switch II	Ras-like; enhanced GTP hydrolysis	–	–	–
D1994A/R1398L	Kinase and GTPase	?	↓↓	↓↓	↓↓
G2019S/T1348N	Kinase and GTPase	Kinase-inactive	↓↓	↓↓	↓↓
G2019S/R1398L	Kinase and GTPase	?	–	↑↑	↑↑
G2019S/K1906M	Kinase	Kinase-inactive	–	–	↓↓
G2019S/D1994A	Kinase	Kinase-inactive	–	–	↓↓
G2019S/D1994N	Kinase	Kinase-inactive	–	–	↓↓
D1994A/R1398L/T1343V	Kinase and GTPase	?	↓↓	↓↓	↓↓
G2019S/R1398L/T1343V	Kinase and GTPase	?	–	–	↑/↑↑

The shading divides functional classes of mutations i.e. GTPase versus kinase, but also single, double and triple mutations.

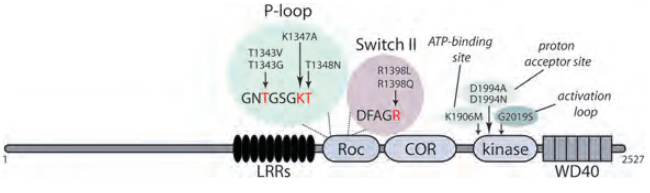

Figure 1. Domain architecture of LRRK2 and the locations of functional GTPase and kinase domain mutations used in this study. Indicated are functional missense mutations within the guanine nucleotide-binding P-loop motif and Switch II catalytic motif within the Roc GTPase domain, and the ATP-binding site, proton-acceptor site and the activation loop of the kinase domain.

that are GTPase-active (WT), GTPase-impaired (T1348N) or GTPase-enhanced (R1398L). As predicted, WT and, to a greater extent, R1398L variants produce a marked time-dependent increase in GTP hydrolysis compared with the T1348N variant over a period of 120 min (Fig. 3B). The residual hydrolysis mediated by the T1348N mutant in this assay may reflect low-level GTPase activity of this mutant, consistent with reduced but not completely impaired GTP binding. For subsequent assays, we monitored GTP hydrolysis over 120 min for comparisons among LRRK2 mutations (Table 1). We find that P-loop mutations (K1347A, T1348N and G2019S/T1348N) markedly impair LRRK2 GTP hydrolysis compared with WT protein (Fig. 2C), consistent with their impaired GTP binding (Fig. 3A). Mutations that alter kinase activity (K1906M, D1994A, D1994N and G2019S) do not significantly influence GTPase activity (Fig. 3C). The R1398L and G2019S/R1398L mutations consistently and significantly enhance GTP hydrolysis (Fig. 3C). We have previously reported that the introduction of Ras-like R1398Q/T1343G mutations into a Roc-COR-kinase domain fragment of LRRK2 (residues 1300–2163) modestly enhances GTP hydrolysis (13); however, in the context of full-length LRRK2, these mutations no longer have a significant effect (Fig. 3C). Importantly, the R1398L/T1343V mutant, analogous to a GTP-locked version of Ras, markedly impairs LRRK2 GTPase activity despite displaying normal GTP binding (Fig. 3A and C). The R1398L/T1343V mutant therefore represents a GTPase-inactive, presumably GTP-locked form of LRRK2. Interestingly, the introduction of the G2019S mutation to the R1398L/T1343V variant (G2019S/R1398L/T1343V) restores normal GTPase activity, suggesting that the effects of the R1398L/T1343V variant on GTPase activity are kinase-dependent (Fig. 3C). Notably, the introduction of the kinase-inactive D1994A mutation has no effect on the diminished GTPase activity of the R1398L/T1343V variant (Fig. 3C). Collectively, we have identified functional mutations within the catalytic Switch II motif that robustly enhance (R1398L) or impair (R1398L/T1343V) the GTPase activity of LRRK2 independent of GTP binding (Table 1). Our data also confirm that P-loop mutations (i.e. K1347A and T1348N) impair the GTP binding and GTP hydrolysis of LRRK2.

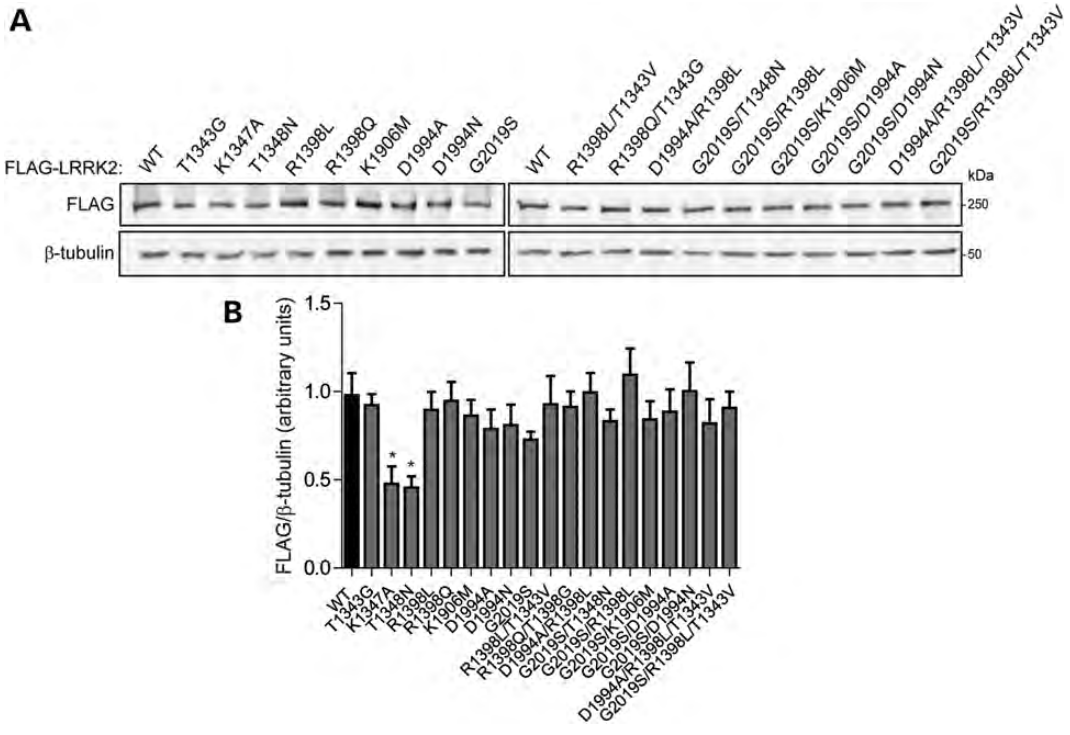

Figure 2. Steady-state protein levels of LRRK2 GTPase domain mutants in HEK-293T cells. (**A**) Western blot analysis of Triton-soluble fractions derived from HEK-293T cells transiently expressing FLAG-tagged human LRRK2 (WT or functional mutants) with anti-FLAG antibody to determine the steady-state levels of LRRK2 or anti-β-tubulin as protein-loading control. Molecular weight markers are indicated in kilodaltons. (**B**) Densitometric analysis of LRRK2 levels normalized to β-tubulin expressed in arbitrary units. Bars represent mean ± SEM ($n = 5–6$ experiments). $^{*}P < 0.05$ compared with WT LRRK2 by one-way ANOVA with the Newman–Keuls *post hoc* analysis.

GTP binding and GTP hydrolysis are required for LRRK2 kinase activity

Having identified GTPase domain mutations that significantly modulate GTPase activity, we next explored the effects of altering GTPase activity on the kinase activity of LRRK2. We first measured LRRK2 autophosphorylation by conducting *in vitro* radioactive kinase assays with immunopurified, soluble full-length LRRK2 variants and [^{33}P]-γ-ATP. As expected, kinase-inactive LRRK2 variants (D1994A and D1994N) dramatically impair, whereas the pathogenic G2019S mutation enhances autophosphorylation activity of LRRK2 compared with the WT protein (Fig. 4A and B). The G2019S/D1994A and G2019S/D1994N variants prevent the G2019S-mediated increase in LRRK2 autophosphorylation, as predicted, since the D1994 site serves as a key catalytic residue of the kinase domain, i.e. the proton acceptor (Fig. 4A and B). P-loop mutants (K1347A, T1348N and G2019S/T1348N) also markedly impair LRRK2 autophosphorylation (Fig. 4A and B), as previously reported (7,10,11), confirming that guanine nucleotide-binding capacity is critically required for kinase activity. The Ras-like mutant, R1398Q/T1343G, fails to influence kinase activity (Fig. 4A and B), consistent with its normal GTP-binding and GTP hydrolysis activities (Fig. 3). Unexpectedly, the R1398L and R1398L/T1343V mutants, which oppositely enhance or impair GTPase activity, respectively (Fig. 3C), significantly reduce the autophosphorylation activity of LRRK2 (Fig. 4A and B) but to a smaller extent than P-loop mutations. However, combining the R1398L and R1398L/T1343V mutations with the G2019S mutation (G2019S/R1398L and G2019S/R1398L/T1343V) does not alter the enhanced LRRK2 autophosphorylation induced by the G2019S mutation (Fig. 4A and B), suggesting that the G2019S variant supersedes the modest effects of these GTPase variants on kinase activity. It should be noted, however, that the G2019S/R1398L/T1343V variant displays normal GTP-binding and hydrolysis activities (Fig. 3), consistent with its lack of effect on the elevated autophosphorylation activity of G2019S LRRK2.

The effects of GTPase and kinase domain mutations were also compared by assessing LRRK2-mediated phosphorylation of LRRKtide, a well-characterized pseudosubstrate peptide of LRRK2 (14). We obtained largely similar results compared with LRRK2 autophosphorylation assays with single or double mutants containing kinase-inactive (K1906M, D1994A, D1994N, G2019S/K1906M, G2019S/D1994A, G2019S/D1994N, D1994A/R1398L and D1994A/R1398L/T1343V) or guanine nucleotide-binding-deficient mutations (K1347A, T1348N and G2019S/T1348N) leading to a dramatic impairment of kinase activity compared with WT LRRK2, whereas the G2019S mutation robustly enhances kinase activity (Fig. 4C). The Ras-like R1398Q/T1343G variant fails to alter LRRK2 kinase activity. Consistent with our autophosphorylation data, the R1398L/T1343V variant significantly reduces LRRK2 kinase activity by ∼60% but to a lesser

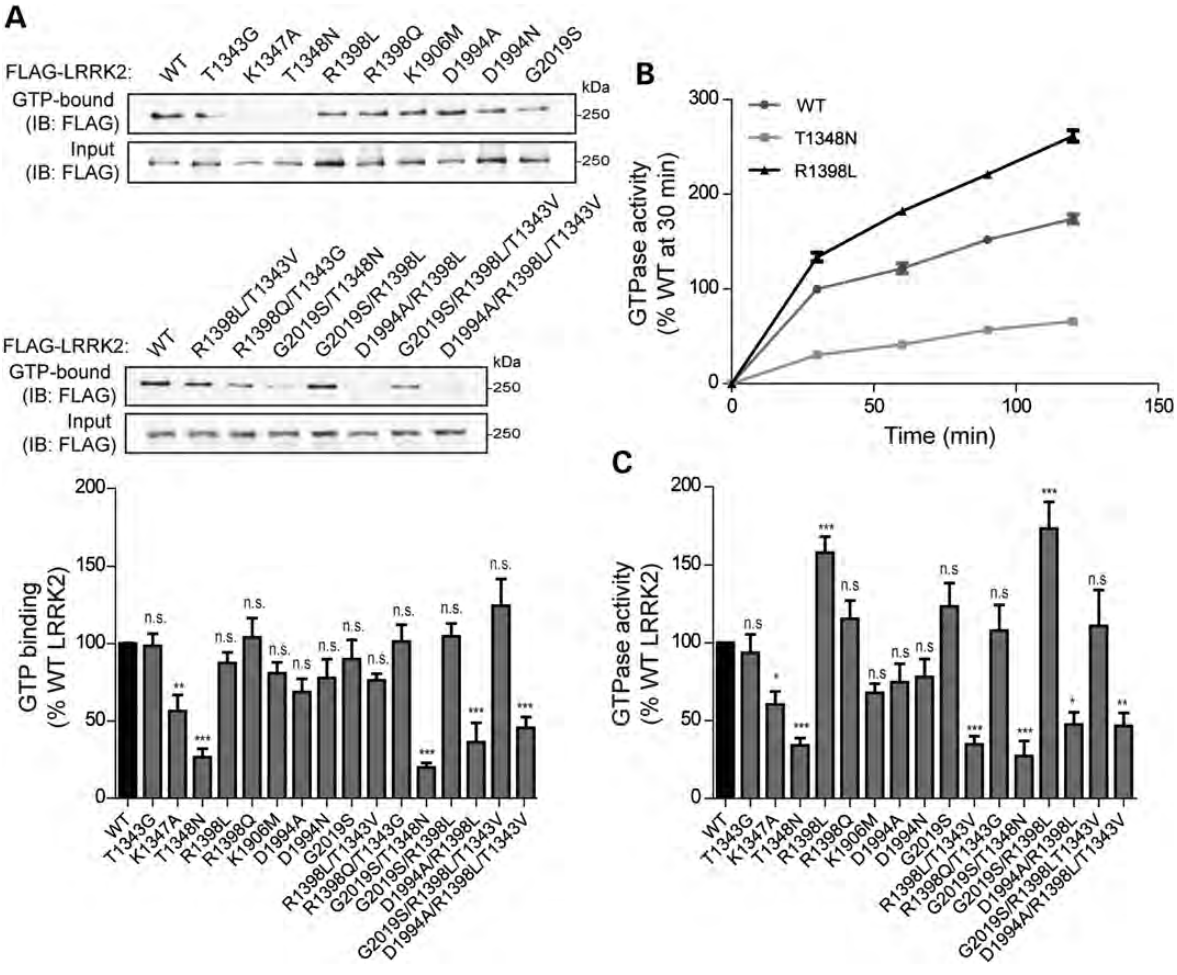

Figure 3. GTPase activity of LRRK2 GTPase domain mutants. (**A**) GTP-binding assay by pull-down with GTP-agarose on HEK-293T cell extracts expressing FLAG-tagged LRRK2 variants. Western blot analysis of GTP-bound fractions (upper panel) and input lysates (lower panel) with anti-FLAG antibody reveals GTP-bound LRRK2. Molecular weight markers are indicated in kilodaltons. Densitometric analysis of GTP-bound LRRK2 normalized to LRRK2 input levels expressed as percentage of WT LRRK2. Bars represent mean ± SEM ($n = 7$ experiments) of GTP binding. $^{**}P < 0.01$ or $^{***}P < 0.001$ compared with WT LRRK2 by one-way ANOVA with the Newman–Keuls *post hoc* analysis. n.s., not significant. (**B**) GTP hydrolysis assay monitoring the release of free γ-phosphate from GTP at 30 min intervals over 120 min mediated by immunopurified FLAG-tagged LRRK2. The guanine nucleotide-binding-deficient T1348N mutant serves as negative control, whereas the GTPase-enhanced R1398L mutant serves as a positive control relative to WT LRRK2. Absorbance values (indicating Pi concentration) for each LRRK2 variant were normalized to the input level of immunoprecipitated (IP) LRRK2 and expressed as percentage of WT LRRK2 after 30 min incubation. Data points represent mean ± SEM ($n = 3$ experiments). (**C**) GTP hydrolysis activity of LRRK2 variants. Assays were incubated for 120 min. GTPase activity was determined by the normalization of absorbance values to IP LRRK2 levels and expressed as percentage of WT LRRK2. Bars represent mean ± SEM ($n \geq 5$ experiments) of GTPase activity. $^{*}P < 0.05$, $^{**}P > 0.01$ or $^{***}P < 0.001$ compared with WT LRRK2 by one-way ANOVA with the Newman–Keuls *post hoc* analysis. n.s., not significant.

extent than P-loop mutations (Fig. 4C). However, the R1398L mutation fails to significantly alter LRRK2 kinase activity (Fig. 4C). The R1398L and R1398L/T1343V variants fail to significantly attenuate the kinase-enhancing effects of the G2019S mutation (Fig. 4C). Taken together, our data suggest that modulating GTPase activity via the R1398L and R1398L/T1343V mutations modestly attenuates kinase activity, suggesting that normal GTPase activity is required in part for the kinase activity of LRRK2. However, modulating GTPase activity is not sufficient to reduce the enhanced kinase activity induced by the pathogenic G2019S mutation. Moreover, guanine nucleotide-binding capacity (i.e. K1347A or T1348N) is critically required for normal LRRK2 kinase activity and for the kinase-enhancing effects of the G2019S mutation.

GTP binding and GTP hydrolysis regulate the GTP-dependent kinase activation of LRRK2

Our LRRK2 autophosphorylation and LRRKtide phosphorylation *in vitro* kinase assays were conducted in the absence of additional guanine nucleotides. LRRK2 kinase activity can be enhanced by the addition of GTP to cell extracts prior to LRRK2 purification, but GTP does not alter kinase activity when added to purified LRRK2 (7,10,11,17), suggesting that GTP-binding capacity rather than direct binding regulates the GTP-dependent kinase activation of LRRK2. In order to explore the effects of functional GTPase domain mutations on the GTP-dependent kinase activation of LRRK2, we conducted *in vitro* radioactive kinase assays to measure LRRKtide phosphorylation using immunopurified, soluble full-length

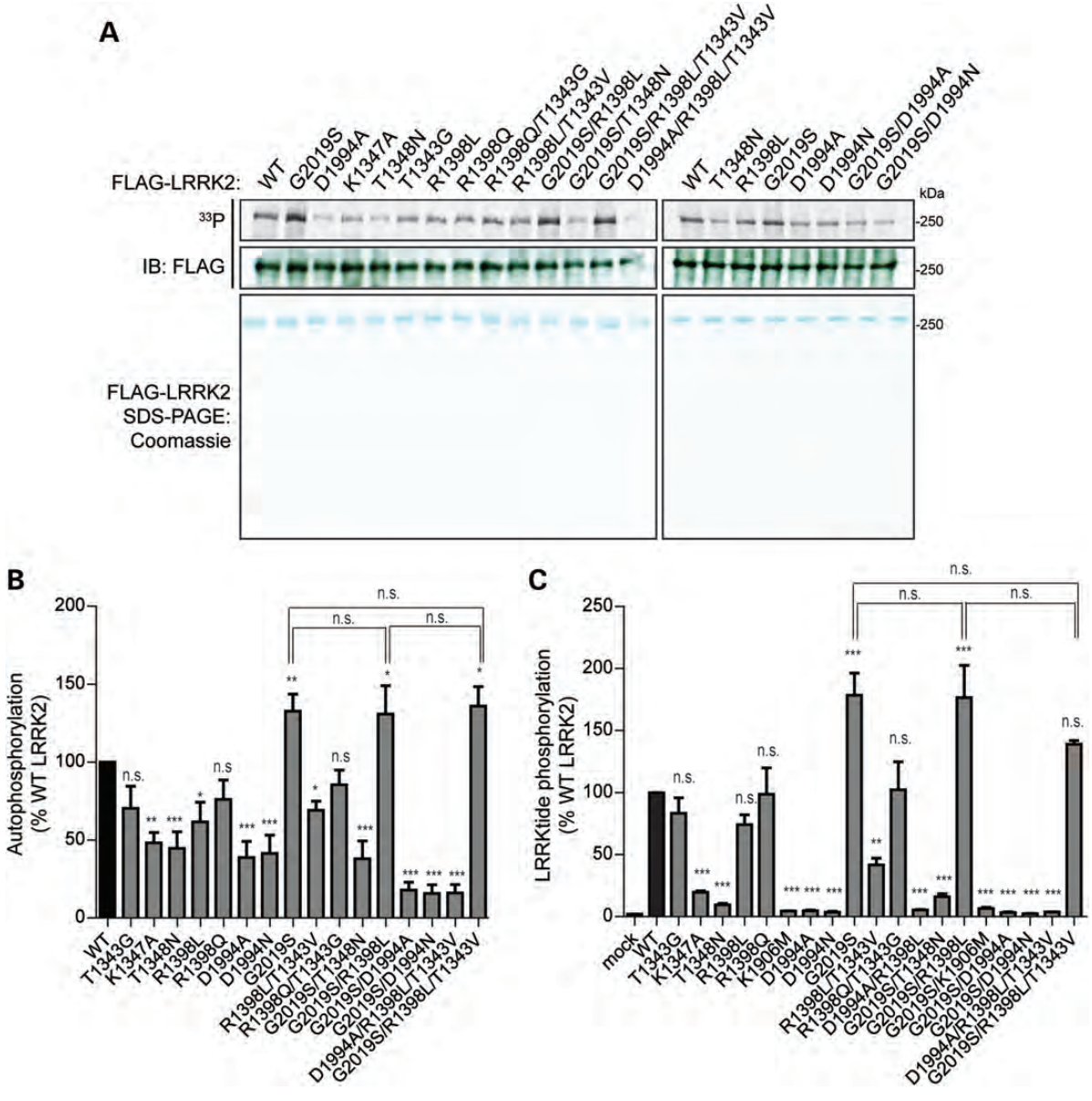

Figure 4. Kinase activity of LRRK2 GTPase domain mutants. (**A**) *In vitro* radioactive kinase assay of LRRK2 autophosphorylation. Autoradiograph (upper panel) of immunopurified FLAG-tagged LRRK2 variants revealing the incorporation of ^{33}P into LRRK2 by autophosphorylation. Western blot analysis with anti-FLAG antibody (middle panel) or staining of equivalent SDS–PAGE gels run in parallel with Coomassie colloidal blue (lower panel) indicates the levels and purity of each immunopurified LRRK2 protein variant. Molecular weight markers are indicated in kilodaltons. (**B**) Normalization of incorporated ^{33}P to LRRK2 input levels by western blotting. Bars represent the mean ± SEM ($n = 4–5$ experiments) of LRRK2 autophosphorylation levels expressed as percentage of WT LRRK2. $^{*}P < 0.05$, $^{**}P < 0.01$ or $^{***}P < 0.001$ compared with WT LRRK2, or as indicated, by one-way ANOVA with the Newman–Keuls *post hoc* analysis. n.s., not significant. (**C**) *In vitro* radioactive kinase assay of LRRK2-mediated phosphorylation of LRRKtide peptide. Incorporation of ^{33}P into LRRKtide peptide (expressed as radioactive counts per minute) was normalized to the levels of immunoprecipitated LRRK2 for each variant, and data were expressed as percent of WT LRRK2. Bars represent the mean ± SEM ($n = 4$ experiments) of LRRKtide phosphorylation levels. $^{**}P < 0.01$ or $^{***}P < 0.001$ compared with WT LRRK2, or as indicated, by one-way ANOVA with the Newman–Keuls *post hoc* analysis. n.s., not significant.

LRRK2 derived from cell extracts treated with GTP or GDP or their non-hydrolyzable analogs βγ-methyleneguanosine 5′-triphosphate (GppCp) or guanosine 5′-[β-thio]diphosphate (GDPβS) at 200 μM, respectively. Treatment with GTP and GppCp enhances the kinase activity of WT LRRK2, whereas treatment with GDP but not GDPβS modestly yet significantly reduces kinase activity compared with untreated LRRK2 (Fig. 5). The guanine nucleotide-binding-deficient T1348N mutant is kinase-inactive and does not respond to guanine nucleotide treatment, as expected (Fig. 5). GTP enhances the kinase activity of WT LRRK2 to a significantly greater extent than non-hydrolyzable GppCp, suggesting that GTP hydrolysis may contribute to kinase activity (Fig. 5). Treatment of the GTPase-enhancing R1398L mutant with GTP or GppCp enhances kinase activity similar to WT LRRK2 but with a proportionally greater effect of GTP over GppCp

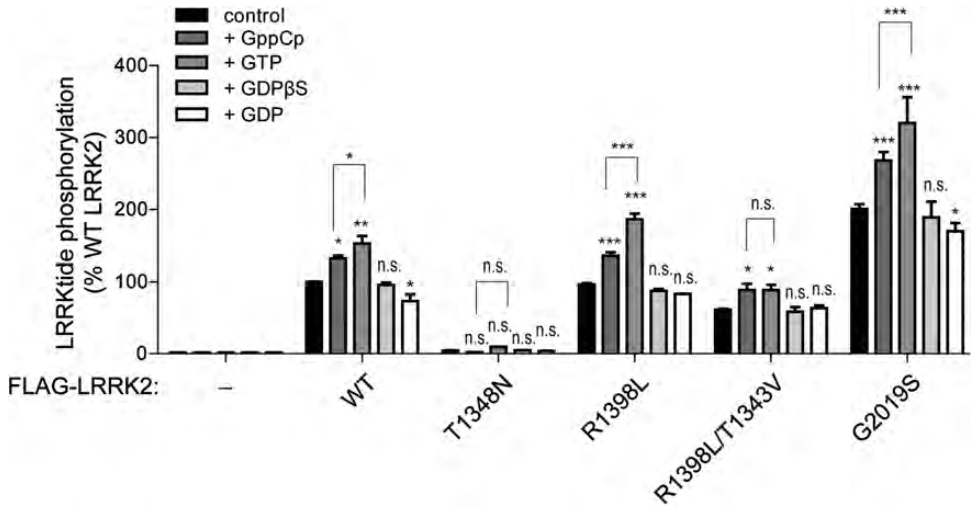

Figure 5. Role of GTPase activity in guanine nucleotide-dependent kinase activation of LRRK2. *In vitro* radioactive kinase assay of LRRKtide peptide phosphorylation with immunopurified FLAG-tagged LRRK2, following treatment with GTP, GppCp, GDP and GDPβS. The graph indicates the LRRK2-mediated incorporation of ^{33}P into LRRKtide peptide normalized to the levels of immunoprecipitated LRRK2 and expressed as a percent of WT LRRK2. Guanine nucleotides (200 μM) were added to HEK-293T cell extracts expressing LRRK2 variants, followed by overnight incubation with anti-FLAG-agarose prior to immunopurification and kinase assays. Bars represent the mean ± SEM ($n = 4–6$ experiments) of the level of LRRKtide phosphorylation. $^{*}P < 0.05$, $^{**}P < 0.01$ or $^{***}P < 0.001$ compared with untreated control, or as indicated, for each LRRK2 variant by one-way ANOVA with the Bonferroni *post hoc* analysis. n.s., not significant.

(Fig. 5), consistent with the enhanced GTP hydrolysis of this mutant promoting kinase activity in response to GTP. In contrast to WT LRRK2, the GTPase-inactive R1398L/T1343V mutant, which exhibits reduced kinase activity, displays an equivalent increase in kinase activity with GTP and GppCp treatment (Fig. 5). The G2019S mutation displays enhanced kinase activity and responds to guanine nucleotides with a profile similar to WT LRRK2 (Fig. 5). Interestingly, enhancing (R1398L) or impairing (R1398L/T1343V) GTPase activity prevents the modest reduction in kinase activity induced by treatment with GDP compared with WT or G2019S LRRK2 (Fig. 5), potentially suggesting that normal GTP hydrolysis activity is required for this effect. Taken together, these data suggest that normal GTP-binding capacity is required for the GTP-dependent kinase activation of LRRK2, whereas GTP hydrolysis is required for the kinase-enhancing effects of GTP compared with non-hydrolyzable GppCp. The GTPase-inactive R1398L/T1343V mutant responds equivalently to GTP and GppCp, thus reflecting the baseline contribution of GTP-binding capacity on kinase activity. Our data suggest that GTP-binding capacity and GTP hydrolysis both contribute in an additive manner to the GTP-dependent kinase activation of LRRK2.

GTP binding but not GTP hydrolysis influences LRRK2 dimerization and Hsp90 binding

LRRK2 is capable of forming a dimeric structure mediated primarily through the COR domain (18–21). Dimerization appears to be critically required for kinase activity since monomeric forms of LRRK2 are kinase-inactive, whereas dimers are kinase-active (19–21). Whether dimerization equivalently regulates GTPase activity or vice versa is not yet clear. We considered whether GTPase domain mutations could influence dimerization and therefore potentially explain their effects on GTPase activity. We first employed size-exclusion chromatography (SEC) to examine the effects of GTPase domain mutations on the formation of LRRK2-native complexes following their immunopurification from HEK-293T cells (Fig. 6A and B). WT LRRK2 elutes over a relatively broad range with the highest signal centered at ∼13 ml and the majority of signal estimated to elute between 440 and 669 kDa compatible with a dimer-sized LRRK2 complex (Fig. 6A and B). Importantly, the R1398L, R1398L/T1343V and R1398Q/T1343G mutants do not obviously influence the hydrodynamic volume of LRRK2 under native conditions relative to WT protein (Fig. 6A and B). Next, we examined the capacity of FLAG-tagged LRRK2 mutants to form hetero-dimers with myc-tagged WT LRRK2 by conducting co-immunoprecipitation (IP) experiments from HEK-293T cells. Myc-tagged WT LRRK2 robustly immunoprecipitates FLAG-tagged WT LRRK2, suggesting the formation of LRRK2 dimeric species (Fig. 6C). Mutants with impaired guanine nucleotide-binding (K1347A, T1348N and G2019S/T1348N) or kinase activity (D1994A and G2019S/D1994A) significantly attenuate the formation of LRRK2 hetero-dimers (Fig. 6C). However, the GTPase-modifying R1398L and R1398L/T1343V mutants exhibit a normal capacity to form LRRK2 hetero-dimers (Fig. 6C). These data suggest that the R1398L and R1398L/T1343V mutants exhibit a normal capacity to form dimeric structures. Furthermore, normal GTP-binding capacity and kinase activity are critically required for LRRK2 dimerization.

The binding of Hsp90 to LRRK2 was recently shown to reflect LRRK2 protein instability, with increased Hsp90 binding correlating with reduced LRRK2 stability and presumably structure (22). To examine the impact of GTPase mutations on LRRK2 stability, we assessed the interaction of

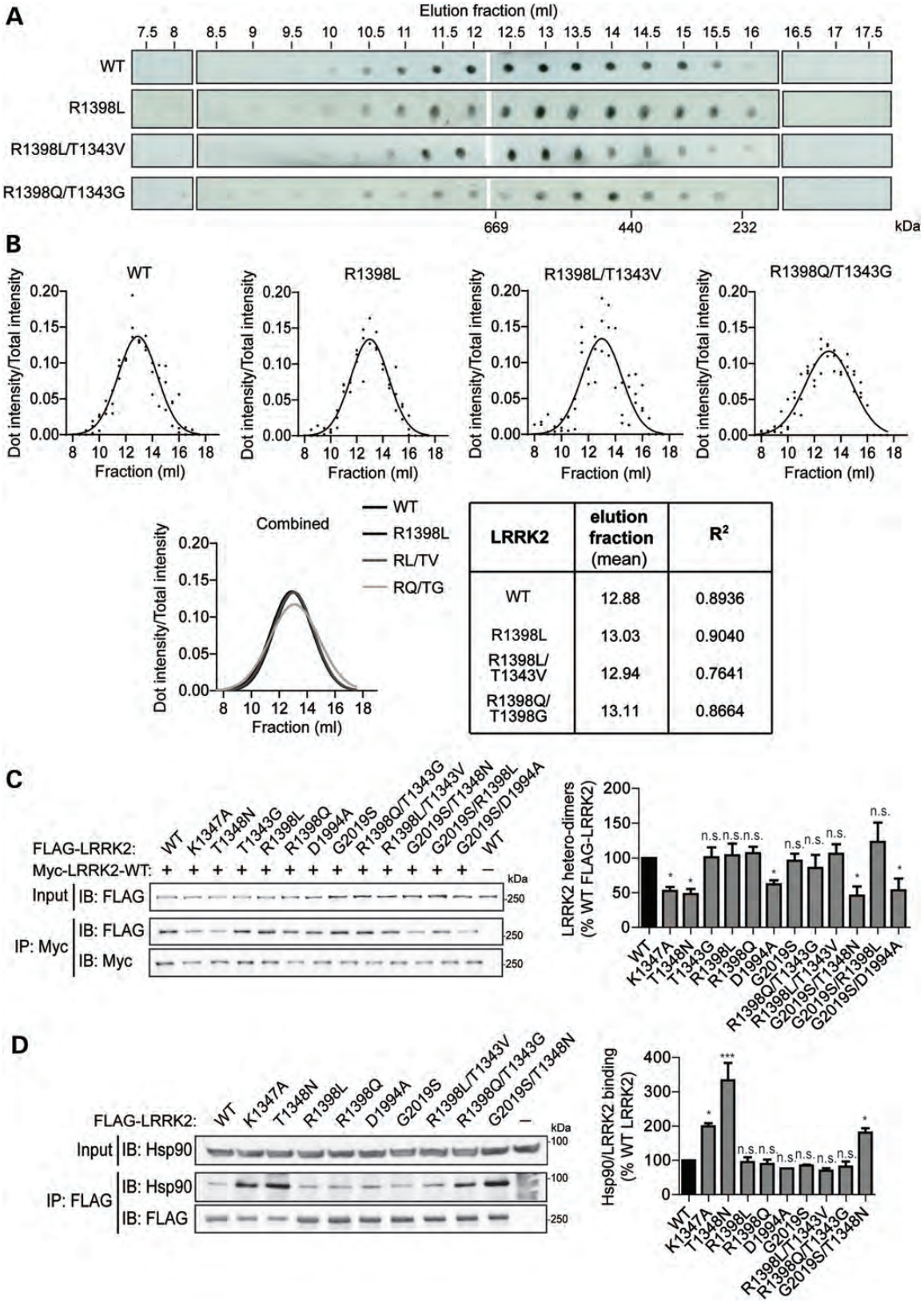

LRRK2	elution fraction (mean)	R^2
WT	12.88	0.8936
R1398L	13.03	0.9040
R1398L/ T1343V	12.94	0.7641
R1398Q/ T1398G	13.11	0.8664

Figure 6. GTP binding but not GTP hydrolysis influences the structural properties of LRRK2. (**A**) SEC elution profiles of immunopurified FLAG-tagged LRRK2 variants derived from HEK-293T cells ($n = 5$ experiments) by western dot-blot analysis with anti-FLAG antibody. Indicated are equivalent quantities of 0.5 ml fractions. The elution of known molecular weight standards is indicated in kilodaltons. (**B**) Densitometric analysis of individual or combined LRRK2 variant elution profiles expressed as the relative signal intensity versus fraction number (ml). The table indicates the mean elution fraction for each LRRK2 variant

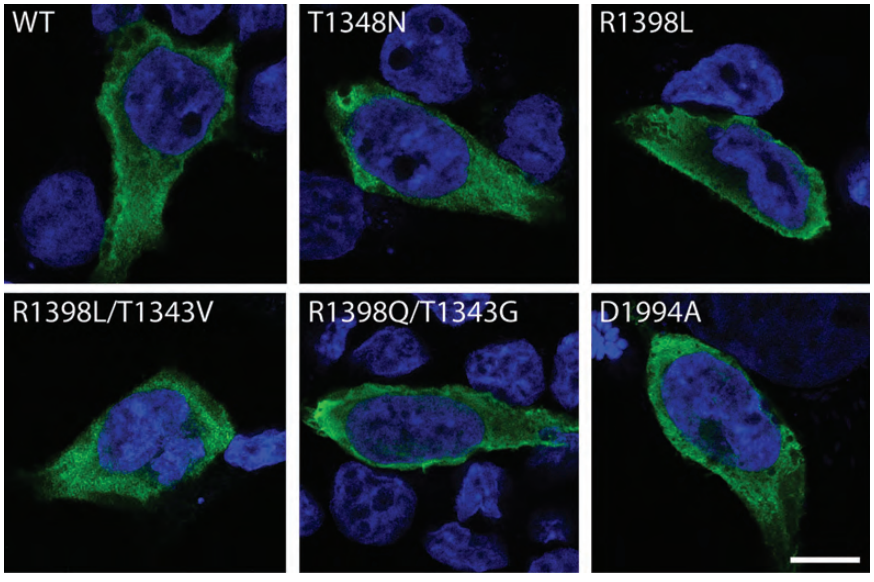

Figure 7. GTPase activity does not alter the subcellular localization of LRRK2. Confocal fluorescence microscopy reveals the diffuse cytoplasmic localization of FLAG-tagged human LRRK2 variants transiently expressed in HEK-293T cells. Staining for LRRK2 (anti-FLAG antibody, green) and nuclei (DAPI, blue) is indicated. Confocal images are taken from a single *z*-plane at 0.1 μm thickness. Images are representative of two independent transfection experiments. Scale bar: 10 μm.

LRRK2 functional mutants with endogenous Hsp90 by co-IP from HEK-293T cells. We find that P-loop mutants (K1347A, T1348N and G2019S/T1348N) display a markedly increased interaction with Hsp90 compared with WT LRRK2 (Fig. 6D), which is consistent with a reduced capacity to form LRRK2 hetero-dimers (Fig. 6C), reduced GTP binding (Fig. 3A) and reduced steady-state protein levels (Fig. 2). In contrast, the GTPase-modifying R1398L and R1398L/T1343V mutants exhibit normal binding to Hsp90 (Fig. 6D). Collectively, our data suggest that the GTPase-modifying mutations, R1398L and R1398L/T1343V, do not influence LRRK2-native complexes, hetero-dimerization or Hsp90 binding, indicating that these variants do not have adverse effects on LRRK2 protein stability or structure. Furthermore, GTPase activity itself does not appear to regulate LRRK2 dimerization or stability. Importantly, GTP-binding capacity critically influences the dimerization and structural properties of LRRK2 protein.

GTP binding and GTP hydrolysis do not regulate the subcellular localization of LRRK2

LRRK2 normally adopts a diffuse cytoplasmic localization pattern in mammalian cells (15,16). To examine the effects of GTPase domain mutations and GTP binding and hydrolysis on the subcellular localization of LRRK2, we assessed HEK-293T cells transiently expressing LRRK2 variants by immunocytochemistry and confocal microscopy. We find that functional variants (R1398L, R1398L/T1343V, R1398Q/T1343G, T1348N and D1994A) generally adopt an equivalent diffuse cytoplasmic distribution pattern similar to WT LRRK2 without evidence of inclusion formation, altered membrane association or subcellular compartmentalization (Fig. 7). Our data suggest that GTP binding and GTP hydrolysis do not regulate the normal cytoplasmic distribution of LRRK2 in mammalian cells.

GTPase activity regulates the effects of LRRK2 on neurite outgrowth

G2019S LRRK2 has been consistently reported to impair the neurite outgrowth of cultured primary neurons in a kinase-dependent manner (12,13,23–25). The contribution of GTPase activity to LRRK2-induced neurite shortening has not been examined. Therefore, we measured the neurite length of primary cortical neurons transiently co-expressing LRRK2 functional mutants and GFP as a marker, using a previously established assay (12). First, we examined the

and R^2 value for each curve fit. (**C**) Co-IP analysis of each FLAG-tagged LRRK2 variant with myc-tagged WT LRRK2 from HEK-293T cells. Western blot analysis of anti-Myc immunoprecipitates (IP; lower panels) or input lysates (upper panel) with anti-FLAG or anti-Myc antibodies is shown. The graph indicates densitometric analysis of LRRK2 hetero-dimer formation (Myc-LRRK2:FLAG-LRRK2). Data represent the level of IP FLAG-LRRK2 normalized to FLAG-LRRK2 input levels and further normalized to IP Myc-LRRK2 levels. Data are expressed as a percent of FLAG-LRRK2-WT. Bars represent the mean ± SEM ($n = 5$ experiments) of hetero-dimer formation. $^{*}P < 0.05$ compared with WT LRRK2 by one-way ANOVA with the Newman-Keuls *post hoc* analysis. n.s., not significant. (**D**) Interaction of endogenous Hsp90 with FLAG-tagged LRRK2 variants in HEK-293T cells by co-IP assay. Western blot analysis of anti-FLAG IP (lower panels) or input lysates (upper panel) with anti-Hsp90 or anti-FLAG antibodies is shown. The graph indicates densitometric analysis of LRRK2/Hsp90 interaction levels. Data represent the level of IP Hsp90 normalized to Hsp90 inputs and further normalized to IP FLAG-LRRK2 levels, and finally expressed as percent of WT LRRK2. Bars represent the mean ± SEM ($n = 3$ experiments) of Hsp90 binding to LRRK2. $^{*}P < 0.05$ or $^{***}P < 0.001$ compared with WT LRRK2 by one-way ANOVA with the Newman–Keuls *post hoc* analysis. n.s., not significant.

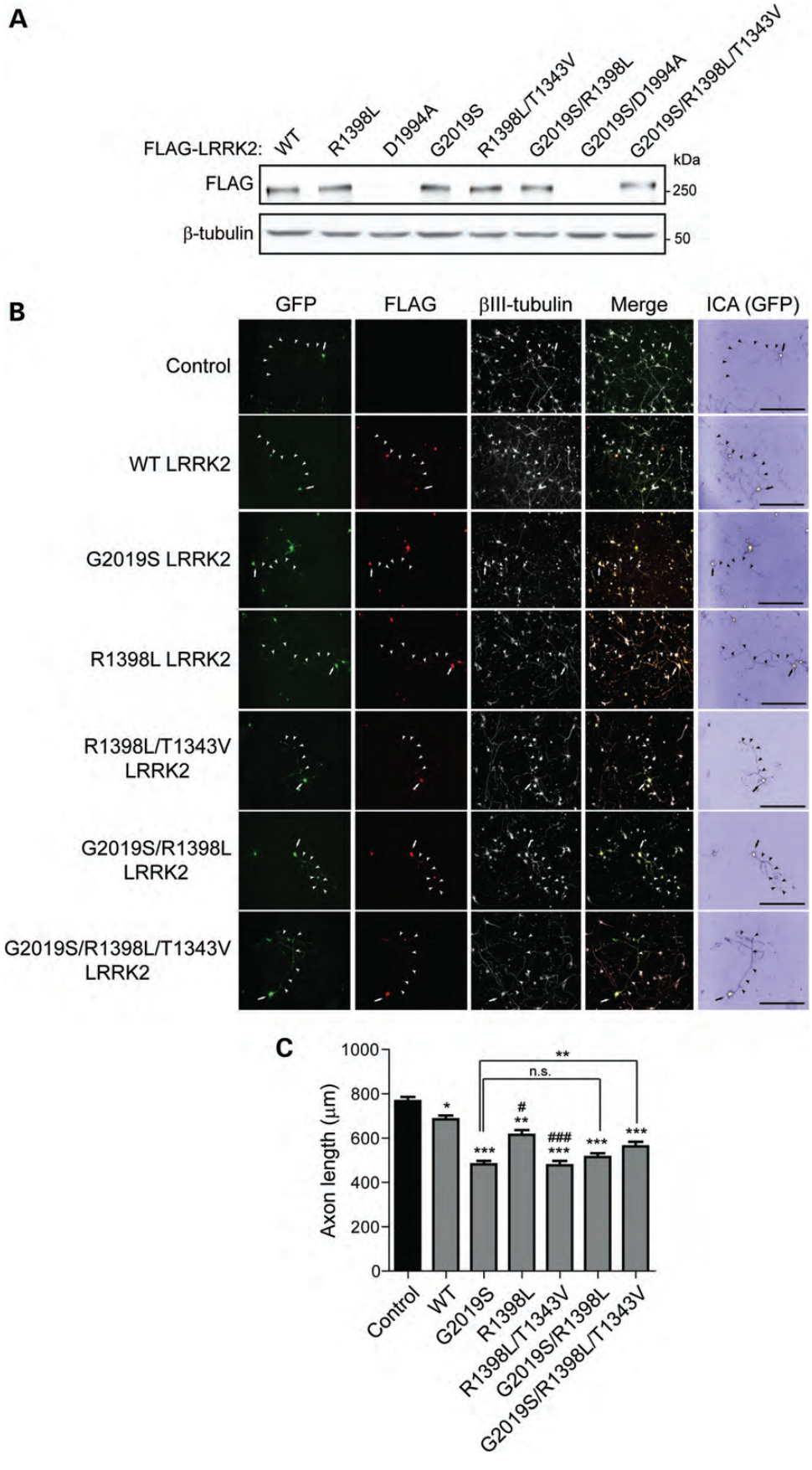
A
FLAG-LRRK2:
WT
R1398L
D1994A
G2019S
R1398L/T1343V
G2019S/R1398L
G2019S/D1994A
G2019S/R1398L/T1343V
kDa
FLAG
250
β-tubulin
50
B
GFP
FLAG
βIII-tubulin
Merge
ICA (GFP)
Control
WT LRRK2
G2019S LRRK2
R1398L LRRK2
R1398L/T1343V LRRK2
G2019S/R1398L LRRK2
G2019S/R1398L/T1343V LRRK2
C
Axon length (μm)
1000
800
600
400
200
0
n.s.
Control
WT
G2019S
R1398L
R1398L/T1343V
G2019S/R1398L
G2019S/R1398L/T1343V

steady-state levels of LRRK2 variants transiently expressed in primary cortical neurons by western blot analysis. Compared with WT LRRK2, kinase-inactive mutants (D1994A and G2019S/D1994A) display markedly reduced protein levels in neurons, whereas the R1398L, R1398L/T1343V, G2019S, G2019S/R1398L and G2019S/R1398L/T1343V variants are detected at normal levels in neurons (Fig. 8A), similar to HEK-293T cells (Fig. 2). We could further demonstrate that kinase-inactive (D1994A and D1994N but not K1906M) and GTP-binding-deficient P-loop (T1348N) mutations reduce the steady-state levels of LRRK2 in cortical neurons presumably due to reduced protein stability (Supplementary Material, Fig. S1). Therefore, we restricted our neurite length analysis to stable variants of LRRK2 with equivalent expression. We find that the G2019S mutation significantly reduces neurite length, whereas WT LRRK2 has a smaller effect compared with control neurons expressing GFP alone (Fig. 8B and C), as previously described (12,23). The GTPase-inactive R1398L/T1343V mutant reduces neurite length to a degree similar to G2019S LRRK2, whereas the GTPase-enhanced R1398L mutant has an intermediate effect between WT and G2019S LRRK2 (Fig. 8B and C). Interestingly, the R1398L mutation is unable to modify the effects of the G2019S mutation on neurite length, whereas the R1398L/T1343V mutation provides a modest yet significant rescue of G2019S-induced neurite shortening (Fig. 8B and C). These neurite length data correlate with the respective effects of R1398L and R1398L/T1343V variants on LRRKtide phosphorylation mediated by G2019S LRRK2 (Fig. 4C), potentially suggesting a kinase-dependent mechanism. Our data suggest that impairing the GTPase activity of LRRK2 (i.e. R1398L/T1343V) promotes neurite shortening but does not further enhance the effects of the G2019S mutation. Furthermore, enhancing the GTPase activity of LRRK2 (i.e. R1398L) is not sufficient to reduce the effect of the G2019S mutation on neurite length. Collectively, our data demonstrate that modulating GTPase activity does not robustly attenuate the inhibitory effect of G2019S LRRK2 on neurite outgrowth, suggesting that the two enzymatic activities of LRRK2 (i.e. GTPase and kinase activity) may act independently of each other to regulate neurite outgrowth.

DISCUSSION

The molecular determinants regulating the GTPase activity of LRRK2 are poorly characterized. Here, we examine the effects of modulating GTPase activity on the enzymatic, biochemical and cellular properties of LRRK2 (Table 1; Supplementary Material, Table S1). A collection of expression constructs were generated containing full-length human LRRK2 with the introduction of various missense mutations located within key functional residues of the GTPase or kinase domains. We identified mutations in the GTPase domain that can either enhance (R1398L) or impair (R1398L/T1343V) GTPase activity without influencing basal GTP binding. Mutations influencing the GTPase activity of LRRK2 modestly attenuated kinase activity, whereas in comparison GTP-binding-deficient mutations dramatically impaired kinase activity. Furthermore, GTP and its non-hydrolyzable analog, GppCp, enhanced the kinase activity of WT LRRK2, whereas the GTPase-inactive variant, R1398L/T1343V, diminished the effects of GTP but not GppCp on kinase activity, suggesting that GTP binding and GTP hydrolysis both contribute to the GTP-dependent kinase activation of LRRK2. Mutations that alter GTPase activity (R1398L or R1398L/T1343V) have negligible effects on LRRK2 dimerization and Hsp90 binding, suggesting that these mutations are likely to exhibit functional rather than destabilizing effects upon LRRK2. In contrast, GTP-binding-deficient mutations (K1347A or T1348N) critically impair the steady-state levels, dimerization and structural properties of LRRK2. Finally, impairing GTPase activity enhances the LRRK2-dependent inhibition of neurite outgrowth, whereas enhancing GTPase activity has an intermediate effect. Importantly, modulating GTPase activity is not sufficient to robustly protect against neurite shortening induced by G2019S LRRK2, suggesting that the kinase and GTPase activities of LRRK2 may act independently to regulate neurite outgrowth. Our data support a complex regulatory interaction between the GTPase and kinase domains of LRRK2 and suggest that GTP-binding capacity and GTP hydrolysis both contribute to the regulation of kinase activity.

Our prior studies in yeast and neuronal models of LRRK2-induced toxicity demonstrated an important role for the GTPase domain in mediating cellular toxicity (13). A kinase-inactive Roc-COR-kinase domain fragment of LRRK2 was shown to induce toxicity in yeast and neurons with mutations that impair GTP binding and hydrolysis (i.e. K1347A and T1348N) leading to enhanced toxicity and mutations that enhance GTP hydrolysis (R1398L and R1398Q/T1343G) attenuating the toxic effects of LRRK2 (13). These previous data suggested that enhancing GTPase activity may have a protective effect against LRRK2-induced toxicity in yeast and cultured neurons at least in the context of a truncated Roc-COR-kinase domain fragment. Motivated by these intriguing observations and the paucity of data concerning the LRRK2 GTPase domain, we sought to explore the functional effects of similar GTPase domain mutations within the context of full-length LRRK2 expressed in mammalian cells. Functional missense mutations generally have minimal effects on the steady-state levels of LRRK2 protein expressed in

Figure 8. GTPase activity regulates the effects of LRRK2 on neurite outgrowth. (**A**) Western blot analysis with anti-FLAG and anti-β-tubulin antibodies of cell extracts derived from rat primary cortical neurons at DIV 7 transiently expressing FLAG-tagged human LRRK2 variants. Molecular weight markers are indicated in kilodaltons. (**B**) Rat primary cortical neurons co-transfected at DIV 3 with FLAG-tagged human LRRK2 variants (or empty control vector) and GFP plasmids at a DNA molar ratio of 10:1. Cultures were fixed at DIV 7. Shown are representative fluorescent micrographs revealing the co-labeling of cortical neurons with GFP, FLAG-LRRK2 and βIII-tubulin for each LRRK2 variant. GFP images were pseudo-colored with ICA to improve the contrast of neuritic processes. Neuronal soma are indicated by arrows, and axonal processes are indicated by arrowheads. Scale bars: 400 μm. (**C**) Analysis of the length of GFP+ neurites from FLAG+/βIII-tubulin+ cortical neurons. Graph represents axon length for each LRRK2 variant in micrometers (mean ± SEM; $n = 3–4$ cultures). $^{*}P < 0.05$, $^{**}P < 0.01$ or $^{***}P < 0.001$ compared with control, or as indicated, and $^{\#}P < 0.05$ or $^{\#\#\#}P < 0.001$ compared with WT LRRK2, by one-way ANOVA with the Newman–Keuls *post hoc* analysis. n.s., not significant.

HEK-293T cells with the notable exception of GTP-binding-deficient mutants (i.e. K1347A or T1348N) which markedly reduce LRRK2 protein levels. Although our data suggest that GTP-binding-deficient mutants are unstable, Switch II motif mutations that modulate GTPase activity have no apparent effects on the steady-state levels of LRRK2. GTP-binding-deficient mutations also diminished LRRK2 hetero-dimerization in co-IP experiments and promoted the interaction with Hsp90, suggesting that they lead to protein instability potentially through altering the structural properties of LRRK2. These data suggest that normal guanine nucleotide-binding capacity is critically required for maintaining LRRK2 dimerization, structure and ultimately stability.

Our data confirm that P-loop motif mutations impair GTP binding similar to previous reports and to equivalent mutations in related small GTPases (7,10,11), whereas Switch II motif mutants (R1398L, R1398L/T1343V and R1398Q/T1343G) exhibit normal GTP binding. Notably, kinase activity was not required for normal GTP binding of LRRK2 despite recent studies revealing multiple sites of autophosphorylation within the GTPase domain (26–29), which questions the relevance of LRRK2 autophosphorylation within cells. We further confirm that P-loop mutations impair GTP hydrolysis, as expected (7,12,13). Furthermore, kinase activity is not required for normal GTP hydrolysis, which raises questions about the exact role of autophosphorylation within the GTPase domain (26–29). Intriguingly, the R1398L and R1398L/T1343V variants exhibit robust yet opposite effects on GTP hydrolysis activity. It is notable that either of the equivalent mutations in small GTPases such as Ras impairs GTP hydrolysis and produces a GTP-locked protein that is constitutively active. Although this appears to be the case for the GTPase-inactive R1398L/T1343V variant of LRRK2, the R1398L mutation alone oppositely enhances GTP hydrolysis. How these effects are mediated is not clear at present, but both mutations presumably alter the structural conformation or flexibility of the GTPase domain but without influencing the basal GTP-binding affinity, dimerization or native complex formation of LRRK2. Determination of the crystal structure of these GTPase-modifying variants within the Roc domain of LRRK2 may help to shed light on the activation mechanism regulating the GTPase domain. ROCO proteins have been postulated to be regulated through a GAD (GTPases activated by dimerization) mechanism of dimerization in *cis* whereby the Roc-COR tandem domain serves as a GAD device, with the Roc domain mediating GTP binding and hydrolysis and the COR domain mediating dimerization (30,31). GAD-containing proteins do not require a GEF or GAP and instead stimulate GTP hydrolysis via dimerization which is usually coupled to the interaction with an effector protein (30). In this context, it is possible that the R1398L/T1343V and R1398L mutations influence the conformational flexibility of the Roc-COR tandem domain, thereby altering the GAD mechanism but without altering dimerization by the COR domain or GTP binding by the Roc domain. Although an intriguing possibility, a GAD mechanism for LRRK2 has not yet been directly demonstrated and will also require reconciliation with the observed effects of ArfGAP1, a GTPase-activating protein, in promoting LRRK2 GTPase activity which would appear to be inconsistent with a GAD-like mechanism (12,32).

The identification of mutations that functionally and oppositely modify the GTPase activity of LRRK2 offered the possibility to explore how GTPase activity contributes to kinase activity and cellular phenotypes of LRRK2. Until now, only the effects of GTP binding upon LRRK2 kinase activity have been explored with GTP binding promoting kinase activity through an indirect mechanism that may involve an unidentified guanine nucleotide-binding protein (7,10,11,17). We demonstrate that enhancing (R1398L) or impairing (R1398L/T1343V) GTP hydrolysis modestly attenuates LRRK2 kinase activity, suggesting a role for normal GTPase activity in maintaining kinase activity. However, in direct comparison, disrupting the GTP-binding capacity (K1347A or T1348N) of LRRK2 led to a robust and consistent impairment of kinase activity. We had originally hypothesized that impairing GTPase activity would prolong the GTP-bound active state of LRRK2 and thereby enhance kinase activity analogous to the mechanism of Ras-mediated activation of Raf kinase. However, this appears not to be the case for the GTPase-impaired R1398L/T1343V variant, whereas the recent demonstration that direct GTP binding to LRRK2 *in vitro* failed to promote its kinase activity collectively suggests that the GTPase and kinase domains of LRRK2 are unlikely to act in a manner analogous to a conventional Ras-Raf mechanism (17). It is possible that GTP hydrolysis *per se* is required for kinase activation through a conformational switching mechanism, with the R1398L and R1398L/T1343V mutations potentially restricting this conformational flexibility. We recently demonstrated that ArfGAP1 can promote LRRK2 kinase activity, further suggesting a requirement of GTP hydrolysis for regulating kinase activity (12). We also examined the effects of GTPase domain variants on the GTP-dependent kinase activation of LRRK2, a mechanism that is thought to be indirect and only occurs in cell extracts prior to LRRK2 purification rather than *in vitro* with purified LRRK2 (7,11,17). Both GTP and its non-hydrolyzable analog, GppCp, enhanced the kinase activity of WT LRRK2, with a greater effect observed for GTP over GppCp. Assuming similar binding affinities for GTP and GppCp to LRRK2, as recently described (17), this finding suggests that GTP binding and GTP hydrolysis both contribute to the GTP-dependent kinase activation of LRRK2 since GppCp is non-hydrolyzable and therefore reflects the contribution of GTP binding only to kinase activation. The GTPase-inactive R1398L/T1343V variant prevented the additional kinase-enhancing effect of GTP over GppCp, further suggesting that GTP hydrolysis contributes to GTP-dependent kinase activation. That guanine nucleotide-binding-deficient mutants (K1347A and T1348N) are kinase-inactive could therefore reflect a combined contribution of impaired GTP binding and GTP hydrolysis. It is worth noting that the GTPase-inactive R1398L/T1343V variant consistently exhibits a modest reduction of basal kinase activity, further supporting a requirement of GTP hydrolysis for maintaining normal kinase activity. Collectively, our data support a contribution of both GTP binding and GTP hydrolysis to regulating the kinase activity of LRRK2.

We have also explored the effects of modulating GTPase activity on biochemical and cellular properties of LRRK2. Since the R1398L/T1343V mutant exhibits impaired GTP hydrolysis and kinase activities, we questioned whether these

mutations could act at a structural level to prevent dimerization and therefore explain their functional effects. The R1398L/T1343V and R1398L mutants could form a normal range of native LRRK2 complexes compared with WT LRRK2, consistent with a dimer-sized complex (i.e. 440–669 kDa) as well as recently described LRRK2 complexes associated with Hsp90 (>669 kDa) (19–22). Therefore, altered GTPase activity most likely does not result from abnormal LRRK2 complex formation including dimerization. The formation of apparent LRRK2 dimers observed by SEC has recently been questioned (33). However, we were able to demonstrate that LRRK2 can form hetero-oligomers by co-IP assays with alternatively tagged proteins that most likely reflect LRRK2 dimers based upon the native LRRK2 complexes revealed by SEC. Although this represents an indirect assay of dimerization, the R1398L/T1343V and R1398L mutants exhibited a normal capacity to form hetero-dimers with WT LRRK2 compared with guanine nucleotide-binding-deficient (K1347A or T1348N) and kinase-inactive (D1994A) mutations which markedly impair dimer formation. Collectively, our data suggest that the GTPase-modifying mutants do not adversely influence LRRK2 dimerization and complex formation, suggesting that (i) the effects of these functional mutations on GTP hydrolysis do not result from altered dimerization and that (ii) GTP hydrolysis itself does not obviously regulate LRRK2 dimerization or complex formation. The R1398L/T1343V and R1398L variants are therefore likely to alter LRRK2 conformation or structural flexibility locally within the GTPase domain in a subtle manner without compromising LRRK2 dimerization or stability. Hsp90 binding to LRRK2 was recently suggested to correlate with a loss of LRRK2 structure, as shown for the kinase-impaired G2385R mutation associated with an increased risk for PD (22). Importantly, the R1398L/T1343V and R1398L variants exhibited normal Hsp90 binding, implying that these LRRK2 variants adopt a normal structure, consistent also with a normal capacity to form LRRK2 complexes and hetero-dimers. Of interest, the guanine nucleotide-binding-deficient mutants, K1347A and T1348N, display increased binding to Hsp90, consistent with their reduced stability and impaired hetero-dimer formation potentially resulting from a loss of LRRK2 structure. The kinase-inactive mutation, D1994A, also exhibited impaired hetero-dimerization consistent with previous reports suggesting a requirement of kinase activity for LRRK2 dimerization (21). Caution is therefore warranted for the interpretation of cellular phenotypes modulated by guanine nucleotide-binding-deficient mutations (i.e. K1347A or T1348N) since they simultaneously impair LRRK2 GTP binding, dimerization and structure, which could all result in attenuated kinase activity. How P-loop mutants lead to unstable forms of LRRK2 is not clear but could potentially result from a loss of structure and dimerization. Our data support the development of strategies for interfering with guanine nucleotide binding via the P-loop motif as an attractive therapeutic mechanism for attenuating the enhanced LRRK2 kinase activity and neuronal toxicity due to the pathogenic G2019S mutation.

LRRK2 can regulate neurite complexity with certain PD-associated mutations leading to reduced neurite length and branching, whereas LRRK2 silencing or deletion has opposing effects (23,24,34). The effects of the G2019S mutation on neurite length are reported to be kinase-dependent (23,25). However, some caution is warranted with such interpretations since we demonstrate that certain kinase-inactive mutations [i.e. D1994A and D1994N, or D1994S (35)] create unstable forms of LRRK2 when expressed in primary neurons compared with mammalian cell lines. We therefore recommend the use of the kinase-inactive K1906M mutation for neuronal culture experiments, which has minimal effects on LRRK2 stability. The contribution of the GTPase domain to LRRK2-induced neurite shortening has not yet been explored. We initially found that the T1348N mutation impairs the stability of LRRK2 protein in cortical neurons, similar to HEK-293T cells, thereby rendering it refractory to further analysis in our neurite length assay. We find that the R1398L/T1343V mutant impaired neurite outgrowth to an extent similar to G2019S LRRK2. The G2019S variant robustly enhances kinase activity but does not influence GTP binding or hydrolysis in the present study, whereas the R1398L/T1343V variant exhibits impaired GTPase activity and reduced kinase activity. Therefore, it is likely that locking LRRK2 in a GTP-bound conformation rather than lowering kinase activity is responsible for the effects of the R1398L/T1343V variant on neurite length. The GTPase-enhanced R1398L mutant, which has inconsistent effects on kinase activity, also induced neurite shortening but to a smaller extent, suggesting that GTPase activity may contribute to the inhibitory effects of LRRK2 on neurite outgrowth in a manner potentially independent of kinase activity. Finally, modulating GTPase activity did not robustly rescue or exacerbate G2019S LRRK2-induced neurite shortening, suggesting that the G2019S mutation may act through a GTPase activity-independent mechanism (i.e. kinase-dependent) or has a dominant effect over GTPase activity. These observations are consistent with the inability of R1398L or R1398L/T1343V mutations to influence the elevated kinase activity of G2019S LRRK2, whereas these GTPase domain mutations alone modestly attenuated kinase activity (Fig. 4). Taken together, these data suggest that GTPase activity is not capable of robustly modifying the inhibitory effects of the G2019S mutation on neurite outgrowth. If one assumes that neurite-shortening phenotypes reflect neuronal toxicity to some extent, then our data suggest that modulating GTP hydrolysis may not provide a promising strategy for inhibiting the neurotoxic actions of the pathogenic G2019S mutation. Our future studies using an adenoviral-mediated rat model of G2019S LRRK2-induced neurodegeneration will hope to clarify the potential neuroprotective effects of genetically modulating GTP-binding and GTP hydrolysis activity (36). It will be important in future studies to explore the contribution of GTPase activity to the neurotoxic actions of other PD-associated LRRK2 mutations (i.e. R1441C, R1441G or Y1699C) located within the Roc-COR domains that exhibit normal kinase activity but a modest impairment of GTP hydrolysis (4,13,14,37).

In summary, we have conducted a comprehensive and comparative analysis of the effects of functional GTPase domain mutations on the enzymatic activity, biochemical and cellular phenotypes of LRRK2 (Table 1; Supplementary Material, Table S1). Importantly, our study demonstrates a critical

requirement of guanine nucleotide binding and, to a lesser extent, GTP hydrolysis for normal kinase activity, and suggests that GTP binding and GTP hydrolysis can both contribute to the GTP-dependent kinase activation of LRRK2. Guanine nucleotide binding further plays a role in maintaining the normal dimerization, structure and stability of LRRK2 protein. Furthermore, GTP hydrolysis activity regulates the LRRK2-dependent inhibition of neurite outgrowth independent of kinase activity, although modulating GTP hydrolysis activity is not sufficient to robustly rescue the effects of pathogenic G2019S LRRK2 on neurite length, consistent with the inability of GTP hydrolysis activity to alter the kinase activity of G2019S LRRK2. Our data further dissects and elucidates the contribution of the GTPase domain to the enzymatic activity, biochemical and cellular properties of LRRK2. Our study suggests that strategies aimed at interfering with guanine nucleotide binding rather than modulating GTP hydrolysis may provide an attractive therapeutic mechanism for inhibiting the elevated LRRK2 kinase activity and neurodegeneration due to the pathogenic G2019S mutation.

MATERIALS AND METHODS

Animals

All animal experiments were approved by the SCAV (Service de la consommation et des affaires vétérinaires) in the Canton de Vaud (Animal authorization No. 2293), and conducted in strict accordance with the European Union directive (2010/63/EU) for the care and use of laboratory animals. Animals were maintained in a pathogen-free barrier facility and exposed to a 12 h light/dark cycle with food and water provided *ad libitum*. Pregnant female Sprague–Dawley rats were obtained from Charles River Laboratories (L'Arbresle Cedex, France), and resulting P0–P1 rats were used for the preparation of post-natal primary cortical cultures.

Expression plasmids, proteins and antibodies

Mammalian expression plasmids containing 3× FLAG-tagged full-length human LRRK2 (WT and G2019S) were kindly provided by Dr Christopher Ross (Johns Hopkins University, Baltimore, MD, USA) (38). Functional missense mutations were introduced in FLAG-tagged LRRK2 by site-directed mutagenesis, using the QuikChange II XL kit (Agilent Technologies, La Jolla, CA, USA) and verified by DNA sequencing. Myc-tagged human WT LRRK2 plasmid was kindly provided by Dr Ted M. Dawson (Johns Hopkins University) (15). As control plasmids, pEGFP-N1 was obtained from Clontech (Mountain View, CA, USA) and pcDNA3.1-myc-his was obtained from Invitrogen (Basel, Switzerland). LRRKtide peptide (RLGRDKYKTLRQIRQ; 97.6% pure by HPLC analysis) was purchased from SignalChem (Richmond, Canada). GTP, GppCp, GDP and GDPβS at >95% purity by HPLC were purchased from Sigma-Aldrich (Buchs, Switzerland). 3× FLAG peptide was purchased from Sigma-Aldrich. The following antibodies were employed: mouse monoclonal anti-FLAG-(M2), anti-FLAG-(M2)-peroxidase and anti-β-tubulin (clone TUB 2.1), and rabbit polyclonal anti-βIII-tubulin (Sigma-Aldrich); anti-c-myc (clone 9E10) and anti-c-myc-peroxidase (Roche Applied Science, Basel, Switzerland); mouse monoclonal anti-Hsp90 (BD Biosciences, Allschwil, Switzerland); peroxidase-coupled anti-mouse IgG (Jackson ImmunoResearch, Inc., West Grove, PA, USA); anti-mouse IgG coupled to AlexaFluor-488 or AlexaFluor-546 and anti-rabbit IgG coupled to AlexaFuor-633 (Invitrogen).

Cell culture and transient transfection

HEK-293T cells were maintained in Dulbecco's modified Eagle's media supplemented with 10% fetal bovine serum and 1× penicillin/streptomycin at 37°C and in a 5% CO_2 atmosphere. Cells were transfected with plasmid DNAs, using X-tremeGENE HP DNA Transfection Reagent (Roche Applied Science) according to the manufacturer's recommendations. Cells were harvested at 48–72 h post-transfection for biochemical assays.

Co-IP assays and western blotting

For co-IP assays, HEK-293T cells were transiently transfected with each plasmid in 10 cm dishes and harvested after 48 h in 1 ml of IP buffer [10 mM Tris–HCl pH 7.5, 150 mM NaCl, 1% NP-40, 1× phosphatase inhibitor cocktail 2 and 3 (Sigma-Aldrich), 1× Complete Mini Protease Inhibitor Cocktail (Roche Applied Sciences)]. Cell lysates were rotated at 4°C for 1 h and soluble fractions were obtained by centrifugation at 17 500*g* for 15 min at 4°C. Soluble fractions were combined with 50 µl of Protein G-Dynabeads (Invitrogen) pre-incubated with mouse anti-FLAG (5 µg; Sigma-Aldrich) or anti-myc (5 µg; Roche Applied Sciences) antibodies and incubated overnight at 4°C. Dynabead complexes were washed three times with IP buffer supplemented with 450 mM NaCl and twice with IP buffer. Immunoprecipitates were eluted by heating at 70°C for 10 min in Laemmli sample buffer (Bio-Rad AG, Reinach, Switzerland) containing 5% 2-mercaptoethanol. IPs and inputs (1% total lysate) were resolved by SDS–PAGE, transferred to Protran nitrocellulose (0.2 µM; Perkin Elmer, Schwerzenbach, Switzerland) and subjected to western blot analysis with appropriate primary and secondary antibodies. Proteins were visualized by enhanced chemiluminescence (ECL; GE Healthcare, Glattbrugg, Switzerland) on a FujiFilm LAS-4000 Luminescent Image Analysis system. The LabImage 1D software (Kapelan Bio-Imaging Solutions, Leipzig, Germany) was used for the quantitation of protein levels by densitometry.

To assess the steady-state protein levels of LRRK2 mutants, transfected HEK-293T cells were lysed in buffer A [1× PBS pH 7.5, 1% Triton X-100, 1× phosphatase inhibitor cocktail 2 and 3 (Sigma-Aldrich), 1× Complete Mini Protease Inhibitor Cocktail (Roche Applied Science)] by rotating for 1 h at 4°C. Clarified lysates were obtained by centrifugation at 17 500*g* for 15 min at 4°C. The detergent-soluble supernatant fraction was quantified by BCA assay (Pierce Biotechnology, Rockford, IL, USA), and proteins (30 µg) were resolved by SDS–PAGE and subjected to western blot analysis with appropriate primary and secondary antibodies.

Immunocytochemistry and confocal microscopy

HEK-293T cells were seeded on glass cover slips in 35 mm dishes at a density of 80 000 cells/dish and transfected with FLAG-tagged LRRK2 variants. At 48 h post-transfection, cells were fixed in 4% paraformaldehyde (PFA) and processed for immunocytochemistry with mouse anti-FLAG antibody and anti-mouse IgG-AlexaFluor-488 antibody and stained with DAPI. Fluorescent images were acquired using a Zeiss LSM 700 inverted confocal microscope (Carl Zeiss AG, Feldbach, Switzerland) with a Plan-Apochromat 63×/1.40 oil objective in *x*, *y* and *z* planes. Images were subjected to deconvolution, using the HuygensPro software (Scientific Volume Imaging, Hilversum, The Netherlands). Representative images are taken from a single *z*-plane at a thickness of 0.1 μm.

Size-exclusion chromatography

HEK-293T cells were lysed in buffer B [20 mM Tris–HCl, pH 7.5, 150 mM NaCl, 1 mM EDTA, 0.5% Tween 20, 1× phosphatase inhibitor cocktail 2 and 3 (Sigma-Aldrich), 1× Complete Mini Protease Inhibitor Cocktail (Roche Applied Science)]. Cleared lysates (1 ml) were incubated with anti-FLAG-M2-agarose beads by rotating overnight at 4°C. Resin complexes were washed with different buffers (2× with 20 mM Tris–HCl, 500 mM NaCl, 0.5% Tween 20; 2× with 20 mM Tris–HCl, 300 mM NaCl, 0.5% Tween 20; 2× with 20 mM Tris–HCl, 150 mM NaCl, 0.5% Tween 20; 2× with 20 mM Tris–HCl, 150 mM NaCl, 0.1% Tween; and 2× with 20 mM Tris–HCl, 150 mM NaCl, 0.02% Tween 20), and LRRK2 proteins were eluted in elution buffer (20 mM Tris–HCl, pH 7.5, 150 mM NaCl, 0.02% Tween 20 and 150 μg/ml of 3× FLAG peptide) for 30 min at 4°C with shaking. Eluted proteins were resolved by SDS–PAGE and stained with Coomassie G-250 to verify protein purity, and LRRK2 content was calculated by densitometry, using a standard curve with bovine serum albumin (BSA). Purified proteins containing equal amounts of each FLAG-LRRK2 variant were injected into an AKTA Purifier FPLC system (GE Healthcare, Italy) and separated using a Superose 6 10/300 column (GE Healthcare, Italy), after equilibration with buffer C (20 mM Tris–HCl, pH 7.5, 150 mM NaCl and 0.07% Tween 20). Pump flow rate was fixed at 0.5 ml/min. Elution volumes of standards were 7.5 ml for Blue Dextran (V_0), 12.37 ml for thyroglobin (669 kDa), 14.21 ml for ferritin (440 kDa) and 15.71 ml for catalase (232 kDa). Each separated fraction obtained by FPLC analysis (1 μl) was spotted on nitrocellulose membranes, incubated with anti-FLAG-peroxidase (Sigma-Aldrich) and subjected to detection with ECL.

GTP binding assay

HEK-293T cells expressing FLAG-tagged LRRK2 variants were lysed in buffer A [1× PBS, pH 7.5, 1% Triton X-100, 1× phosphatase inhibitor cocktail 2 and 3 (Sigma-Aldrich), 1× Complete Mini Protease Inhibitor Cocktail (Roche Applied Science)] by rotating for 1 h at 4°C. Soluble fractions were incubated with 25 μl of guanosine 5′-triphosphate–agarose (Sigma-Aldrich) by rotating for 2 h at 4°C. Agarose beads were washed three times with buffer A and once with 1× PBS. GTP-bound fractions were eluted in Laemmli buffer containing 5% 2-mercaptoethanol and heating at 70°C for 10 min. GTP-bound fractions and inputs lysates (1% total lysate) were resolved by SDS–PAGE and subjected to western blot analysis with anti-FLAG-peroxidase antibody.

GTP hydrolysis assay

GTP hydrolysis assay was performed as previously described (12,13) by measuring the release of free γ-phosphate (Pi) from GTP, using the high-sensitivity colorimetric GTPase assay kit (Innova Biosciences, Cambridge, UK). To establish time curves for LRRK2 GTPase activity, HEK-293T cells transiently expressing FLAG-tagged LRRK2 variants (WT, T1348N and R1398L) were lysed in phosphate-free lysis buffer [10 mM Tris–HCl, pH 7.5, 150 mM NaCl, 1% NP-40, 1× phosphatase inhibitor cocktail 2 and 3 (Sigma-Aldrich), 1× Complete Mini Protease Inhibitor Cocktail (Roche Applied Science)]. Following centrifugation at 17 500*g* for 15 min, supernatant fractions were subjected to IP with 2.5 μg of anti-FLAG antibody pre-incubated with 25 μl of Protein G-Dynabeads (Invitrogen) by rotating at 4°C overnight. As control for protein contamination, mock-transfected HEK-293T cell lysates were subjected to IP with anti-FLAG antibody. Dynabeads were washed five times with lysis buffer and once with 0.5 M Tris–HCl, pH 7.5, then resuspended in 100 μl of 0.5 M Tris–HCl, pH 7.5, and finally subjected to GTP hydrolysis assays in 96-well plates in assay buffer containing 0.25 mM GTP. Reactions were incubated for 30, 60, 90 and 120 min at room temperature according to the manufacturer's recommendations. Assay samples were measured for absorbance at 635 nm, and Pi concentration was determined from standard curves. The control absorbance value for the mock IP FLAG sample was deducted from the absorbance values obtained for each LRRK2 sample. FLAG IP samples (5 μl of total) were subjected to western blotting with anti-FLAG antibody to confirm LRRK2 immunopurification. The levels of each IP LRRK2 variant was quantified by densitometry and used to normalize LRRK2-mediated Pi release in each experiment. Data were expressed as a percent of Pi release due to WT LRRK2 after 30 min. Subsequent LRRK2 GTPase assays were conducted as described earlier with incubation for 120 min at room temperature, with GTPase activity (Pi release) expressed as a percent of WT LRRK2.

In vitro kinase assays

Autophosphorylation assay

For LRRK2 autophosphorylation, transfected HEK-293T cells were lysed, subjected to IP with anti-FLAG-agarose, and LRRK2 proteins were eluted with 3× FLAG peptide as described earlier. Eluted proteins were resolved by SDS–PAGE and stained with Coomassie G-250 (Bio-Rad) to verify protein purity, and LRRK2 content was calculated by densitometry, using a standard curve with BSA. Autophosphorylation reactions were performed in kinase buffer (25 mM Tris–HCl, pH 7.5, 5 mM β-glycerophosphate, 2 mM dithiothreitol, 0.1 mM Na_3VO_4, 10 mM $MgCl_2$) in the presence

of [^{33}P]-γ-ATP (2 μCi/reaction; Perkin Elmer, MA, USA) and 5 μM cold ATP (Sigma-Aldrich) at 30°C for 1 h in a final volume of 25 μl. Reactions were terminated with 4× Laemmli buffer and by boiling at 95°C for 10 min. Autophosphorylation reaction samples were resolved on 4–16% SDS–PAGE pre-cast gels (Invitrogen) and transferred to PVDF membranes. Incorporated radioactivity was detected by autoradiography and the same membranes were probed with anti-FLAG antibody and western blot detection as a protein-loading control. Relative LRRK2 autophosphorylation was determined by densitometric analysis of ^{33}P autoradiograph signals for LRRK2 normalized to LRRK2 protein levels.

LRRKtide phosphorylation assay

To measure LRRKtide phosphorylation, HEK-293T cells were lysed, subjected to IP with anti-FLAG-agarose, and LRRK2 proteins were eluted with 3× FLAG peptide and quantified as described earlier. For treatment with GTP, GppCp, GDP and GDPβS, guanine nucleotides (200 μM) were added to cell lysates immediately prior to incubation with anti-FLAG-agarose, followed by rotation overnight at 4°C. For LRRKtide phosphorylation assay, LRRKtide peptide (400 μM) was added to standard kinase reactions, as described earlier. Reaction samples were terminated by the addition of 8 μl of 0.5 M EDTA and samples were applied to P81 phosphocellulose paper (Whatman, Opfikon, Switzerland). P81 squares were dried, washed three times with 75 mM phosphoric acid (Sigma-Aldrich) and incorporated ^{33}P into LRRKtide peptide was detected by scintillation counting. LRRKtide phosphorylation levels were normalized to the levels of LRRK2 protein determined by western blotting and densitometry.

Primary neuronal cultures and neurite length assays

Primary neuronal cultures

Primary cortical neurons were prepared from Sprague–Dawley P0–P1 rats by stereoscopically isolating the cerebral cortices and dissociation by digestion in media containing papain (20 U/ml, Sigma-Aldrich) and mechanical trituration. Cells were plated in 35 mm dishes on glass cover slips coated with poly-D-lysine (20 ng/ml; BD Biosciences) and mouse laminin (33 μg/ml; Invitrogen) and cultured in Neurobasal media containing B27 supplement (2% w/v), L-glutamine (500 μM) and penicillin/streptomycin (100 U/ml) (Invitrogen).

Neurite length assay

Primary cortical neurons were co-transfected at DIV 3 with FLAG-tagged LRRK2 variants and GFP plasmids at a 10:1 DNA molar ratio (4 μg of total DNA per 35 mm dish), using Lipofectamine 2000 reagent (Invitrogen). At DIV 7, cultures were fixed with 4% PFA and processed for immunocytochemistry, using mouse anti-FLAG antibody (Sigma-Aldrich), rabbit anti-βIII-tubulin (Sigma-Aldrich), anti-mouse IgG-AlexaFluor-546 and anti-rabbit IgG-AlexaFluor-633 antibodies (Invitrogen). Fluorescent images were acquired using an EVOS inverted fluorescence digital microscope (Advanced Microscopy Group, Bothell, WA, USA) with a ×10 objective. GFP images were pseudo-colored with ICA1 using the NIH ImageJ software to improve the contrast of neuritic processes, and used for neurite length measurements. The length of GFP-positive axonal processes from FLAG-positive cortical neurons (βIII-tubulin-positive) was measured using the line tool function of the ImageJ software by an investigator blinded to each condition. Only neurons that had extended neurites were measured, whereas neurons without processes were excluded from the analysis. For each experiment, axonal processes from 30 GFP-positive neurons randomly sampled across five cover slips from at least three independent experiments were measured.

Statistical analysis

Data were analyzed by one-way ANOVA with the Newman–Keuls multiple comparison test or the Bonferroni *post hoc* test. $P < 0.05$ was considered significant. Fitting curves of SEC fractions were obtained by Gaussian regression fit analysis.

SUPPLEMENTARY MATERIAL

Supplementary Material is available at *HMG* online.

ACKNOWLEDGEMENTS

The authors would like to thank Klodjan Stafa (EPFL) and the EPFL BioImaging and Optics facility for assistance with confocal microscopy and image processing.

Conflict of Interest statement. None declared.

FUNDING

This work was supported by funding from the Swiss National Science Foundation (grant nos 127478 and 144063 to D.J.M.), the EPFL (D.J.M.), the University of Sassari (A.B.), Michael J. Fox Foundation for Parkinson's Research (E.G.), Rientro dei Cervelli Program (lncentivazione alla mobilita di studiosi stranieri e italiani residenti all'estero) from the Italian Ministry of Education, University and Research (E.G.), the Fondazione CARIPLO (grant no. 2011 0540 to E.G.) and the Fondazione Telethon (grant GGP12237 to E.G.). L.C. is a Michael J. Fox Foundation research fellow.

REFERENCES

1. Healy, D.G., Falchi, M., O'Sullivan, S.S., Bonifati, V., Durr, A., Bressman, S., Brice, A., Aasly, J., Zabetian, C.P., Goldwurm, S. *et al.* (2008) Phenotype, genotype, and worldwide genetic penetrance of LRRK2-associated Parkinson's disease: a case-control study. *Lancet Neurol.*, **7**, 583–590.
2. Paisán-Ruiz, C., Jain, S., Evans, E.W., Gilks, W.P., Simón, J., van der Brug, M., de Munain, A.L., Aparicio, S., Gil, A.M., Khan, N. *et al.* (2004) Cloning of the gene containing mutations that cause PARK8-linked Parkinson's disease. *Neuron*, **44**, 595–600.
3. Zimprich, A., Biskup, S., Leitner, P., Lichtner, P., Farrer, M., Lincoln, S., Kachergus, J., Hulihan, M., Uitti, R.J., Calne, D.B. *et al.* (2004) Mutations in LRRK2 cause autosomal-dominant parkinsonism with pleomorphic pathology. *Neuron*, **44**, 601–607.
4. Tsika, E. and Moore, D.J. (2012) Mechanisms of LRRK2-mediated neurodegeneration. *Curr. Neurol. Neurosci. Rep.*, **12**, 251–260.

5. Marin, I. (2006) The Parkinson disease gene LRRK2: evolutionary and structural insights. *Mol. Biol. Evol.*, **23**, 2423–2433.
6. Marin, I., van Egmond, W.N. and van Haastert, P.J. (2008) The Roco protein family: a functional perspective. *FASEB J.*, **22**, 3103–3110.
7. Ito, G., Okai, T., Fujino, G., Takeda, K., Ichijo, H., Katada, T. and Iwatsubo, T. (2007) GTP binding is essential to the protein kinase activity of LRRK2, a causative gene product for familial Parkinson's disease. *Biochemistry*, **46**, 1380–1388.
8. Lewis, P.A., Greggio, E., Beilina, A., Jain, S., Baker, A. and Cookson, M.R. (2007) The R1441C mutation of LRRK2 disrupts GTP hydrolysis. *Biochem. Biophys. Res. Commun.*, **357**, 668–671.
9. Li, X., Tan, Y.C., Poulose, S., Olanow, C.W., Huang, X.Y. and Yue, Z. (2007) Leucine-rich repeat kinase 2 (LRRK2)/PARK8 possesses GTPase activity that is altered in familial Parkinson's disease R1441C/G mutants. *J. Neurochem.*, **103**, 238–247.
10. Smith, W.W., Pei, Z., Jiang, H., Dawson, V.L., Dawson, T.M. and Ross, C.A. (2006) Kinase activity of mutant LRRK2 mediates neuronal toxicity. *Nat. Neurosci.*, **9**, 1231–1233.
11. West, A.B., Moore, D.J., Choi, C., Andrabi, S.A., Li, X., Dikeman, D., Biskup, S., Zhang, Z., Lim, K.-L., Dawson, V.L. *et al.* (2007) Parkinson's disease-associated mutations in LRRK2 link enhanced GTP-binding and kinase activities to neuronal toxicity. *Hum. Mol. Genet.*, **16**, 223–232.
12. Stafa, K., Trancikova, A., Webber, P.J., Glauser, L., West, A.B. and Moore, D.J. (2012) GTPase activity and neuronal toxicity of Parkinson's disease-associated LRRK2 is regulated by ArfGAP1. *PLoS Genet.*, **8**, e1002526.
13. Xiong, Y., Coombes, C.E., Kilaru, A., Li, X., Gitler, A.D., Bowers, W.J., Dawson, V.L., Dawson, T.M. and Moore, D.J. (2010) GTPase activity plays a key role in the pathobiology of LRRK2. *PLoS Genet.*, **6**, e1000902.
14. Jaleel, M., Nichols, R.J., Deak, M., Campbell, D.G., Gillardon, F., Knebel, A. and Alessi, D.R. (2007) LRRK2 phosphorylates moesin at threonine-558: characterization of how Parkinson's disease mutants affect kinase activity. *Biochem. J.*, **405**, 307–317.
15. West, A.B., Moore, D.J., Biskup, S., Bugayenko, A., Smith, W.W., Ross, C.A., Dawson, V.L. and Dawson, T.M. (2005) Parkinson's disease-associated mutations in leucine-rich repeat kinase 2 augment kinase activity. *Proc. Natl Acad. Sci. USA*, **102**, 16842–16847.
16. Greggio, E., Jain, S., Kingsbury, A., Bandopadhyay, R., Lewis, P., Kaganovich, A., van der Brug, M.P., Beilina, A., Blackinton, J., Thomas, K.J. *et al.* (2006) Kinase activity is required for the toxic effects of mutant LRRK2/dardarin. *Neurobiol. Dis.*, **23**, 329–341.
17. Taymans, J.M., Vancraenenbroeck, R., Ollikainen, P., Beilina, A., Lobbestael, E., De Maeyer, M., Baekelandt, V. and Cookson, M.R. (2011) LRRK2 kinase activity is dependent on LRRK2 GTP binding capacity but independent of LRRK2 GTP binding. *PLoS One*, **6**, e23207.
18. Deng, J., Lewis, P.A., Greggio, E., Sluch, E., Beilina, A. and Cookson, M.R. (2008) Structure of the ROC domain from the Parkinson's disease-associated leucine-rich repeat kinase 2 reveals a dimeric GTPase. *Proc. Natl Acad. Sci. USA*, **105**, 1499–1504.
19. Berger, Z., Smith, K.A. and LaVoie, M.J. (2010) Membrane localization of LRRK2 is associated with increased formation of the highly active LRRK2 dimer and changes in its phosphorylation. *Biochemistry*, **49**, 5511–5523.
20. Greggio, E., Zambrano, I., Kaganovich, A., Beilina, A., Taymans, J.-M., Daniëls, V., Lewis, P., Jain, S., Ding, J., Syed, A. *et al.* (2008) The Parkinson disease-associated leucine-rich repeat kinase 2 (LRRK2) is a dimer that undergoes intramolecular autophosphorylation. *J. Biol. Chem.*, **283**, 16906–16914.
21. Sen, S., Webber, P.J. and West, A.B. (2009) Dependence of leucine-rich repeat kinase 2 (LRRK2) kinase activity on dimerization. *J. Biol. Chem.*, **284**, 36346–36356.
22. Rudenko, I.N., Kaganovich, A., Hauser, D.N., Beylina, A., Chia, R., Ding, J., Maric, D., Jaffe, H. and Cookson, M.R. (2012) The G2385R variant of leucine-rich repeat kinase 2 associated with Parkinson's disease is a partial loss-of-function mutation. *Biochem. J.*, **446**, 99–111.
23. MacLeod, D., Dowman, J., Hammond, R., Leete, T., Inoue, K. and Abeliovich, A. (2006) The familial parkinsonism gene LRRK2 regulates neurite process morphology. *Neuron*, **52**, 587–593.
24. Parisiadou, L., Xie, C., Cho, H.J., Lin, X., Gu, X.-L., Long, C.-X., Lobbestael, E., Baekelandt, V., Taymans, J.-M., Sun, L. *et al.* (2009) Phosphorylation of Ezrin/Radixin/Moesin proteins by LRRK2 promotes the rearrangement of actin cytoskeleton in neuronal morphogenesis. *J. Neurosci.*, **29**, 13971–13980.
25. Ramsden, N., Perrin, J., Ren, Z., Lee, B.D., Zinn, N., Dawson, V.L., Tam, D., Bova, M., Lang, M., Drewes, G. *et al.* (2011) Chemoproteomics-based design of potent LRRK2-selective lead compounds that attenuate Parkinson's disease-related toxicity in human neurons. *ACS Chem. Biol.*, **6**, 1021–1028.
26. Gloeckner, C.J., Boldt, K., von Zweydorf, F., Helm, S., Wiesent, L., Sarioglu, H. and Ueffing, M. (2010) Phosphopeptide analysis reveals two discrete clusters of phosphorylation in the N-terminus and the Roc domain of the Parkinson-disease associated protein kinase LRRK2. *J. Proteome Res.*, **9**, 1738–1745.
27. Greggio, E., Taymans, J.M., Zhen, E.Y., Ryder, J., Vancraenenbroeck, R., Beilina, A., Sun, P., Deng, J., Jaffe, H., Baekelandt, V. *et al.* (2009) The Parkinson's disease kinase LRRK2 autophosphorylates its GTPase domain at multiple sites. *Biochem. Biophys. Res. Commun.*, **389**, 449–454.
28. Kamikawaji, S., Ito, G. and Iwatsubo, T. (2009) Identification of the autophosphorylation sites of LRRK2. *Biochemistry*, **48**, 10963–10975.
29. Webber, P.J., Smith, A.D., Sen, S., Renfrow, M.B., Mobley, J.A. and West, A.B. (2011) Autophosphorylation in the leucine-rich repeat kinase 2 (LRRK2) GTPase domain modifies kinase and GTP-binding activities. *J. Mol. Biol.*, **412**, 94–110.
30. Wittinghofer, A. and Vetter, I.R. (2011) Structure-function relationships of the G domain, a canonical switch motif. *Annu. Rev. Biochem.*, **80**, 943–971.
31. Gasper, R., Meyer, S., Gotthardt, K., Sirajuddin, M. and Wittinghofer, A. (2009) It takes two to tango: regulation of G proteins by dimerization. *Nat. Rev. Mol. Cell Biol.*, **10**, 423–429.
32. Xiong, Y., Yuan, C., Chen, R., Dawson, T.M. and Dawson, V.L. (2012) ArfGAP1 is a GTPase activating protein for LRRK2: reciprocal regulation of ArfGAP1 by LRRK2. *J. Neurosci.*, **32**, 3877–3886.
33. Ito, G. and Iwatsubo, T. (2012) Re-examination of the dimerization state of leucine-rich repeat kinase 2: predominance of the monomeric form. *Biochem. J.*, **441**, 987–994.
34. Plowey, E.D., Cherra, S.J., Liu, Y.-J. and Chu, C.T. (2008) Role of autophagy in G2019S-LRRK2-associated neurite shortening in differentiated SH-SY5Y cells. *J. Neurochem.*, **105**, 1048–1056.
35. Herzig, M.C., Kolly, C., Persohn, E., Theil, D., Schweizer, T., Hafner, T., Stemmelen, C., Troxler, T.J., Schmid, P., Danner, S. *et al.* (2011) LRRK2 protein levels are determined by kinase function and are crucial for kidney and lung homeostasis in mice. *Hum. Mol. Genet.*, **20**, 4209–4223.
36. Dusonchet, J., Kochubey, O., Stafa, K., Young, S.M. Jr, Zufferey, R., Moore, D.J., Schneider, B.L. and Aebischer, P. (2011) A rat model of progressive nigral neurodegeneration induced by the Parkinson's disease-associated G2019S mutation in LRRK2. *J. Neurosci.*, **31**, 907–912.
37. Greggio, E. and Cookson, M.R. (2009) Leucine-rich repeat kinase 2 mutations and Parkinson's disease: three questions. *ASN Neuro*, **1**, e00002.
38. Smith, W.W., Pei, Z., Jiang, H., Moore, D.J., Liang, Y., West, A.B., Dawson, V.L., Dawson, T.M. and Ross, C.A. (2005) Leucine-rich repeat kinase 2 (LRRK2) interacts with parkin, and mutant LRRK2 induces neuronal degeneration. *Proc. Natl Acad. Sci. USA*, **102**, 18676–18681.